Journal of Alloys and Compounds 513 (2012) 373–377

Contents lists available at SciVerse ScienceDirect

Journal of Alloys and Compounds

journal homepage: www.elsevier.com/locate/jallcom

Fabrication of nanopowders by high energy ball milling and low temperature sintering of Mg_2SiO_4 microwave dielectrics

Lin Cheng[a,*], Peng Liu[a], XiaoMing Chen[a], WenCheng Niu[a], GuoGuang Yao[a], Cheng Liu[a], XiaoGang Zhao[a], Qian Liu[a], HuaiWu Zhang[b]

[a] *College of Physics and Information Technology, Shaanxi Normal University, Xi'an 710062, China*

[b] *The Key Laboratory of Electronic Thin Film and Integrated Device, University of Electronic Science and Technology of China, Chengdu 610054, China*

ARTICLE INFO

Article history:
Received 19 May 2011
Received in revised form 15 October 2011
Accepted 18 October 2011
Available online 25 October 2011

Keywords:
Mechanical alloying
Nanostructured materials
Ceramics
X-ray diffraction

ABSTRACT

Mg_2SiO_4 nanopowders were prepared from MgO and SiO_2 mixtures by using a high energy ball milling method, combined with subsequent calcination at low temperatures. After milling for 30 h, pure phase Mg_2SiO_4 nanopowders with an average grain size of 147.4 nm were obtained at 850 °C, 300 °C lower than that required by a conventional solid state reaction process. Mg_2SiO_4 ceramics sintered at a low temperature of 1075 °C showed almost full density and excellent microwave dielectric properties ($\varepsilon_r = 7.2$, $Q \times f = 193{,}800$ GHz, $\tau_f = -58$ ppm/°C).

1. Introduction

Recently, much attention has been paid to the development of microwave telecommunication technologies because of the increased requirements for microwave applications. These applications demand microwave substrate materials with high quality factor ($Q \times f$) to achieve high selectivity, low dielectric constant (ε_r) to reduce the delay time of electronic signal, and nearly zero temperature coefficient of resonant frequency (τ_f) for frequency stability. Promising candidates include as Mg_2SiO_4 ($Q \times f = 40{,}000$–$240{,}000$ GHz, $\varepsilon_r = 6$–7, $\tau_f = -60$ ppm/°C) [1,2], Al_2O_3 ($Q \times f = 680{,}000$ GHz, $\varepsilon_r = 10$, $\tau_f = -55$ ppm/°C) [3,19], Mg_2SnO_4 ($Q \times f = 55{,}100$ GHz, $\varepsilon_r = 8.41$, $\tau_f = -62$ ppm/°C) [11], $Ba(Zn_{1/3}Ta_{2/3})O_3$ ($Q \times f = 120$ THz) [23], $Li_2MgTi_3O_8$ ($Q \times f = 36{,}200$ GHz, $\varepsilon_r = 26$, $\tau_f = -2$ ppm/°C) [24] and other microwave dielectrics materials [25–33]. Among these materials, forsterite Mg_2SiO_4 has attracted a great attention with low dielectric constant and loss tangent.

In MgO–SiO_2 binary systems, there are Mg_2SiO_4 and $MgSiO_3$ phases. A number of methods to synthesize Mg_2SiO_4 powders, such as solid state reaction, sol–gel, and aqueous methods [1,5,6,10,14,17]. Usually, with a solid state reaction method for preparation of Mg_2SiO_4 ceramics, $MgSiO_3$ as a secondary phase is almost inevitable, a major cause of serious damage to the microwave dielectric properties of Mg_2SiO_4 ceramics. Various efforts have been employed to synthesize single Mg_2SiO_4 phase such as sol–gel and other chemical methods [5,12]. By introducing nonstoichiometry and adjusting the Mg/Si ratios, Song et al. obtained pure phase Mg_2SiO_4 ceramics with an enhanced $Q \times f$ value (114,730 GHz), but the sintering temperature of the ceramics was as high as 1350 °C [7]. How to obtain pure Mg_2SiO_4 phase and sintering the ceramics at low sintering temperatures is still a challenging issue.

High energy ball milling (HEBM) is a simple and efficient method for preparing nanometer powders and HEBM of starting powder is effective to enhance the sintering kinetics [13]. This is because they have nanometer particle size and very high homogeneity, leading to a reduced phase formation temperature [8]. Furthermore, compared with soft chemical methods [5], HEBM is suitable for mass production. In this study, we prepared Mg_2SiO_4 powders via HEBM method. Single phase Mg_2SiO_4 ceramics were obtained at lower temperatures from the HEBM derived mixtures. The effects of HEBM on phase transformation, sintering behavior, and microwave dielectric properties of the Mg_2SiO_4 ceramics were reported.

2. Experimental procedures

Commercially available MgO (99.99% purity) and SiO_2 (99.99% purity) powders were used as the starting materials with the nominal composition of Mg_2SiO_4. The mixtures were milled for 5–30 h with a Fritsch Vario-Planetary HEBM system in air. Tungsten carbide vial with diameter of 80 mm and tungsten carbide balls with diameter of 10 mm were used as milling medium. The rotational speed of vials and

---

* Corresponding author.
E-mail address: chenglin@stu.snnu.edu.cn (L. Cheng).

0925-8388/$ – see front matter © 2011 Elsevier B.V. All rights reserved.
doi:10.1016/j.jallcom.2011.10.051

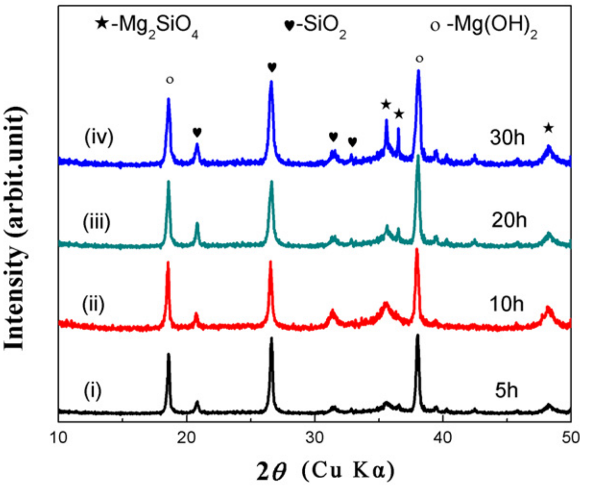

Fig. 1. XRD patterns of the MgO–SiO$_2$ mixtures milled for different times.

ball-to-powder-to-deionized water mass ratio were 300 rpm and 20:1:1.5, respectively. After drying, the milled powders were calcined at 500–900 °C for 3 h at 3 °C/min in air. The calcined powders were milled again for 10 h. After drying, the powders mixed with 5 wt.% PVA as binder and granulated. The granulated powders were pressed into pellets with cylindrical shape under the pressure of 170 MPa and sintered at 1000–1100 °C for 3 h in air.

Reaction behaviors of the milled powders were investigated by using thermal gravimetric and differential thermal analysis (TG/DTA) (SDT Q600 V8.0 Build 95, American) with heating rate of 10 °C/min in air from room temperature to 1100 °C. Phase constituents of the samples were characterized by using X-ray diffraction (XRD) (Rigaku D/max 2250, Japan) (40 kV, 50 mA) with Cu K$_\alpha$ radiation. Microstructures and grain size of the powders and ceramics were examined by using scanning electron microscopy (SEM) (Quanta 200, Germany) and a laser particle size analyzer (BI-90Plus, America), respectively. Densities of the ceramics were measured by using the Archimedes methods. Dielectric behaviors at microwave frequency were measured by the TE$_{01\delta}$ shielded cavity method with a network analyzer (8720ES, Agilent, USA) and a temperature chamber (Delta Design 9023, USA). The τ_f value was calculated by the following formula [20]:

$$\tau_f = \frac{f_{60} - f_{20}}{f_{60}(60 - 20)} \times 10^6 (\text{ppm}/{}^\circ\text{C}) \qquad (1)$$

where f_{60} and f_{20} were the TE$_{01\delta}$ resonant frequencies at 60 and 20 °C, respectively.

3. Results and discussion

Fig. 1 shows XRD patterns of the powders milled for different times. After milling for 5 h, MgO disappeared and $Mg(OH)_2$ was detected (chemical reaction between MgO and hot water (150–200 °C)) [18]. With increasing milling time, forsterite Mg_2SiO_4 phase content with relatively weak diffraction intensity increases. As the milling time was increased to 30 h, two strongest peaks of Mg_2SiO_4 phase were obviously detected. Hence, Mg_2SiO_4 forsterite could be formed by mechanochemical reaction, even though the pure phase could not be synthesized by HEBM alone.

Fig. 2 shows TG/DTA curves of the powders milled for 30 h. The DTA curve exhibits one endothermic peak starting at 270 °C, which is accompanied by a weight loss of approximately 0.8% due to the decomposition of $Mg(OH)_2$ [15]. The exothermic peak starting at 570 °C is related to the formation of forsterite phase, so calcination temperatures were determined to be higher than 570 °C [16].

Fig. 3 shows XRD patterns of the 30 h HEBM powders and those being calcined at various temperatures for 3 h. As shown in Fig. 3(i) for the uncalcined powders, the main diffraction peaks are attributed to SiO_2 and $Mg(OH)_2$ with Mg_2SiO_4 as a minor phase. Calcined at 600 °C (Fig. 3(ii)), the peak intensity of Mg_2SiO_4 is obviously enhanced, in agreement with the DTA analysis shown in Fig. 2. Further increasing calcined temperatures, forsterite Mg_2SiO_4 phase content increases with a disappearance of SiO_2 and $Mg(OH)_2$ phases. As the calcining temperature is increased up to 850 °C

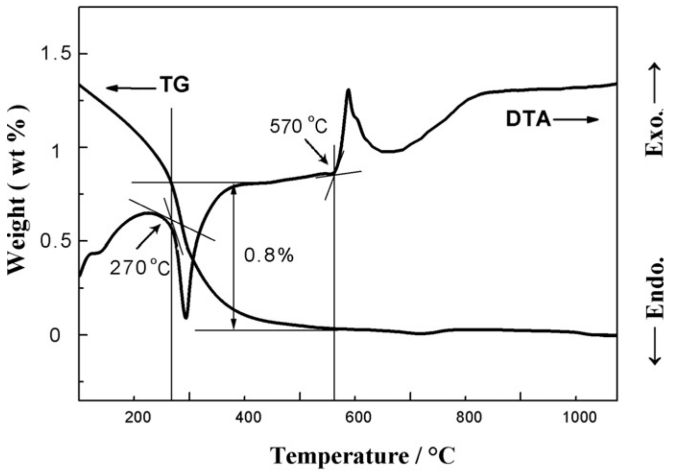

Fig. 2. TG/DTA curves of the MgO–SiO$_2$ mixtures milled for 30 h.

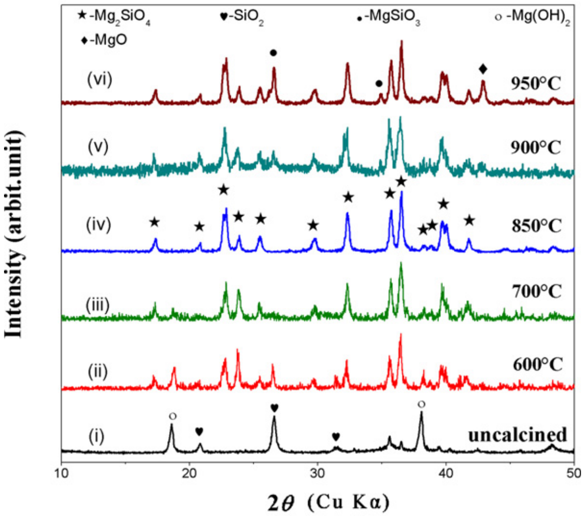

Fig. 3. XRD patterns of the MgO–SiO$_2$ mixtures milled for 30 h and calcined at different temperatures for 3 h.

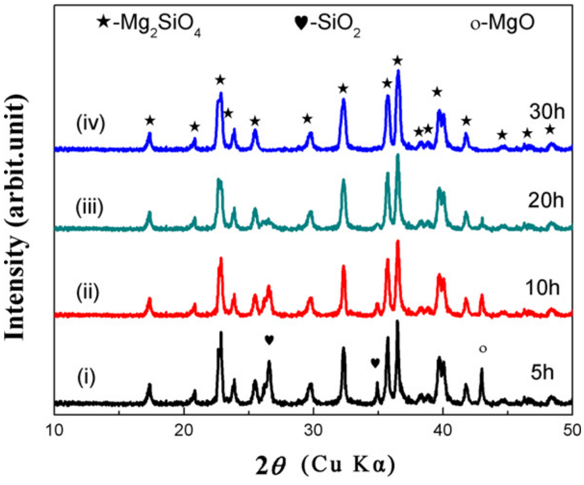

Fig. 4. XRD patterns of the MgO–SiO$_2$ mixtures milled for different times and calcined at 850 °C for 3 h.

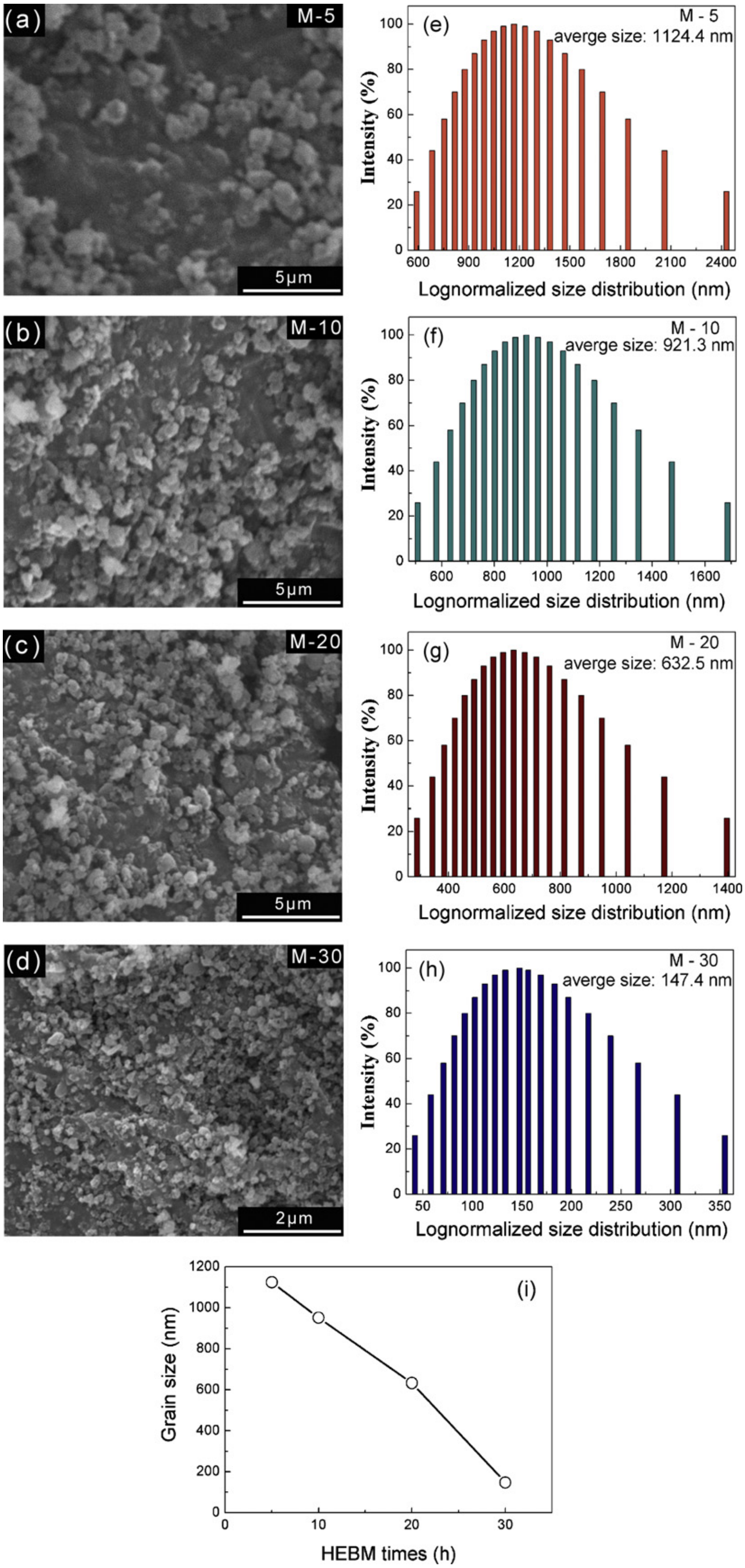

Fig. 5. Representative SEM micrographs (a–d), particle size distribution of the MgO and SiO_2 mixtures calcined at 850 °C for 3 h (e–h), average particle size as a function of milling times (i).

(Fig. 3(iv)), a pure phase forsterite is obtained. However, calcination above 900 °C resulted in the appearance of $MgSiO_3$ and MgO phases (Fig. 3(v and vi)), related to the decomposition of Mg_2SiO_4 at elevated temperatures [21]. Hence XRD analysis indicated that the Mg_2SiO_4 purity forsterite phase is obtained by mechanochemical reaction using HEBM for 30 h and calcined at 850 °C which is 300 °C lower than that required by a conventional solid state reaction technique [2,7]. Therefore, calcination temperature of forsterite Mg_2SiO_4 was determined as 850 °C.

Fig. 4 shows XRD patterns of the powders milling at different times, and calcined at 850 °C dwelling for 3 h. For the calcined powders milled for 5 h (Fig. 4(ii)), Mg_2SiO_4 appears as dominant phase with SiO_2 and MgO as minor phases [18]. As the milling time was increased to 30 h (Fig. 4(iv)), a single phase Mg_2SiO_4 with a well-developed XRD pattern is obtained. Therefore, HEBM is an effective approach to reduce the phase formation temperature of Mg_2SiO_4 phase [8], meanwhile increasing milling time is beneficial for obtaining the pure Mg_2SiO_4 phase.

Fig. 5 shows representative SEM micrographs (Fig. 5(a–d)) and particle size distribution of the MgO and SiO_2 mixtures calcined at 850 °C for 3 h (Fig. 5(e–h)) and average particle size as a function of different milling times (Fig. 5(i)). As shown in Fig. 5(i), particle size decreases with increasing milling time. Compared with the conventional ball milling method, HEBM leads to a reduced average particle size and a narrowed size distribution [9,22]. Similar result was ever reported for various ferroelectric compounds and alloys [8]. For the powders calcined at 850 °C as the HEBM time increasing from 5 h to 30 h, the average particle size is reduced gradually from 1124.4 (Fig. 5(e)) to 147.4 nm (Fig. 5(h)), in agreement with the SEM micrographs shown in Fig. 5(a–d). Particle size of powders milled for 30 h calcined at 850 °C is 120–150 nm (Fig. 5(d) and (h)). Therefore, the MgO–SiO_2 mixtures milled 30 h and calcined at 850 °C was employed to fabricate Mg_2SiO_4 ceramics.

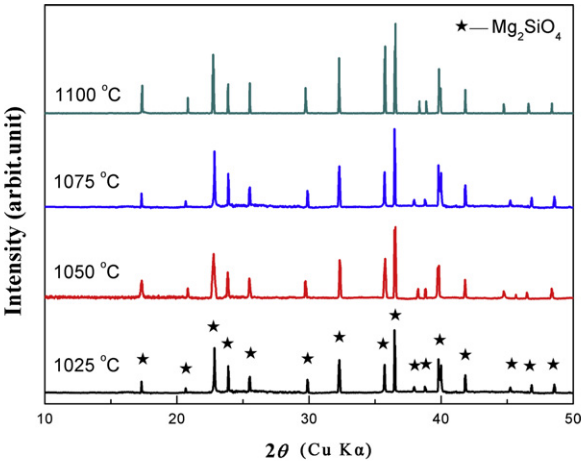

Fig. 6. XRD patterns of the Mg_2SiO_4 ceramics sintered at 1025–1100 °C.

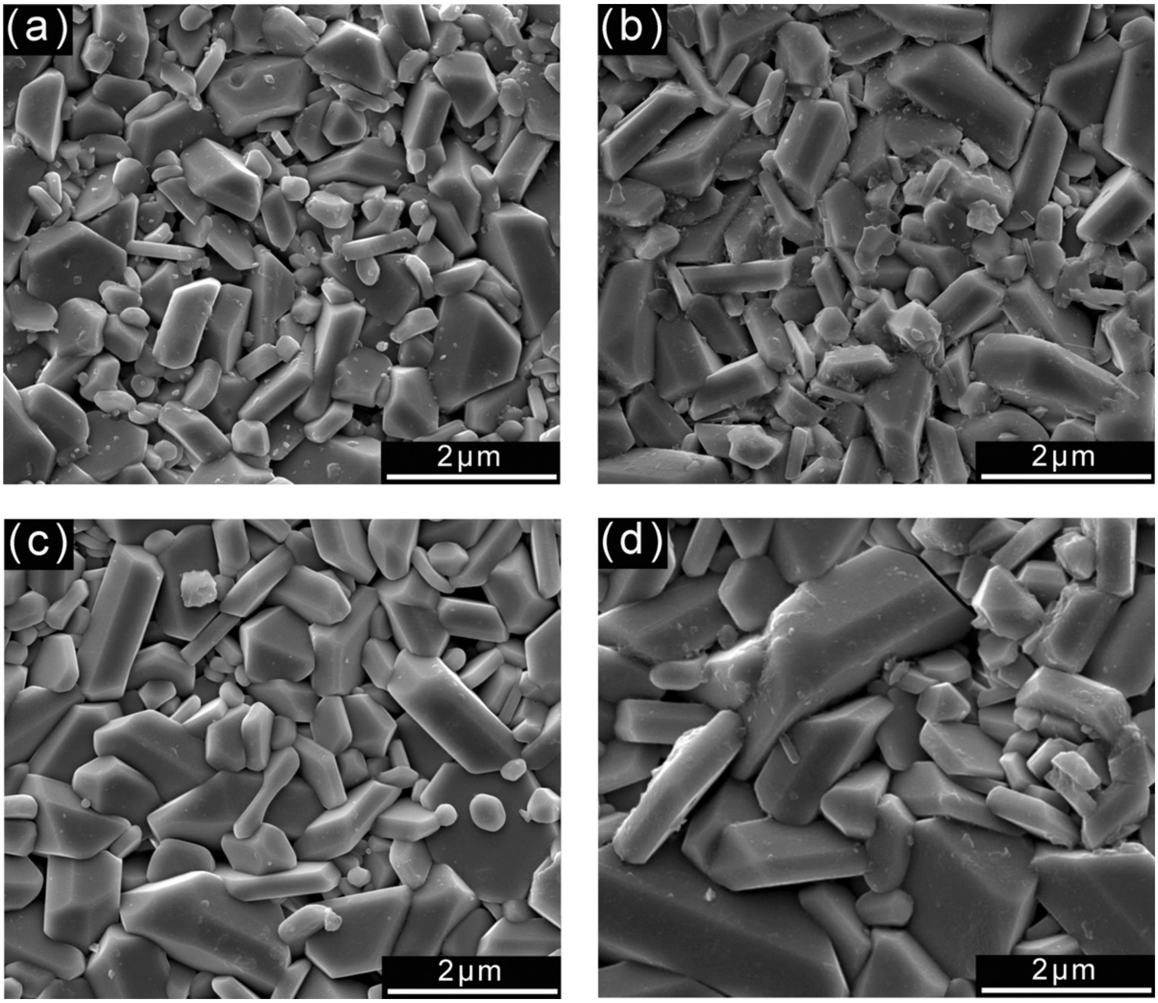

Fig. 7. SEM surface microstructures of the forsterite ceramics sintered at (a) 1025 °C, (b) 1050 °C, (c) 1075 °C, and (d) 1100 °C for 3 h in air.

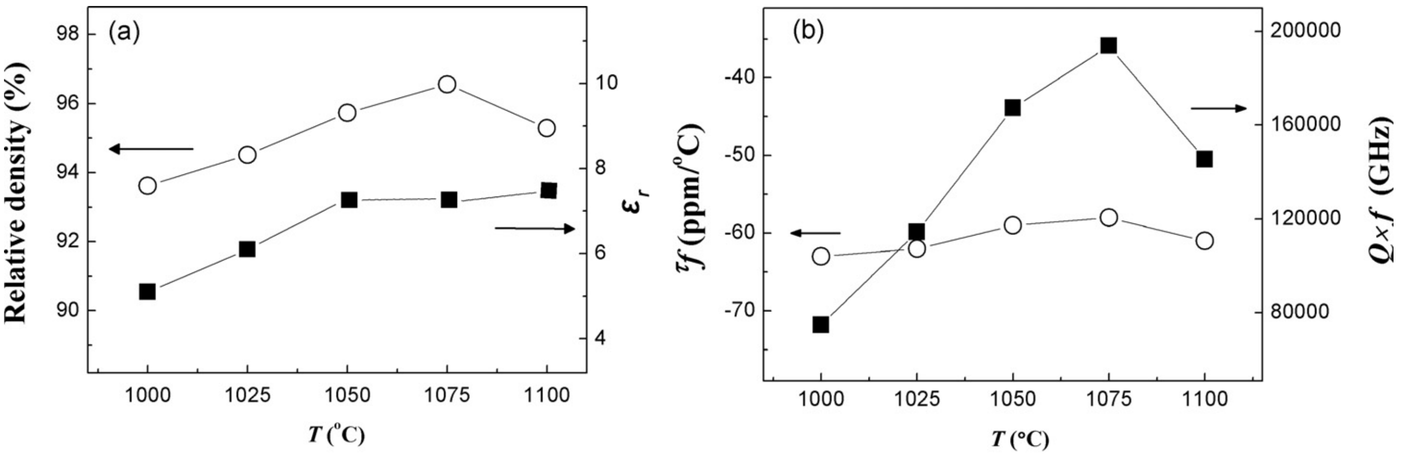

Fig. 8. (a) Relative density, dielectric constant (ε_r), (b) quality factor ($Q \times f$) and τ_f of the Mg_2SiO_4 ceramics as a function of sintering temperatures.

Fig. 6 shows XRD patterns of the Mg_2SiO_4 ceramics sintered at 1025 °C to 1100 °C. As shown in Fig. 6, all the ceramics sintered at 1025–1100 °C are to be a single Mg_2SiO_4 phase. Fig. 7 shows SEM surface microstructures of the Mg_2SiO_4 ceramics as-sintered at 1025–1100 °C. All samples have dense microstructures, but for sample sintered at 1100 °C an abnormal growth of grain size was appeared (Fig. 7(d)), which will make a decrease of $Q \times f$ values. Fig. 8(a) shows relative density and dielectric constant (ε_r) of the Mg_2SiO_4 ceramics from the 30 h milled powders sintered at different temperatures. The relative densities increase to their maximum values as the sintering temperatures increase from 1000 °C to 1075 °C, and then decrease slightly with further increasing temperatures to 1100 °C, due to the abnormal grain growth shown in Fig. 7(d). The optimum sintering temperature (1075 °C) is much (300 °C) lower than other's works reported in recent years [1,7]. Relative density of the sample sintered at 1075 °C reaches to 96.56%, same level comparing with previous reports of the materials prepared by the other methods [4]. With increasing sintering temperatures from 1000 to 1075 °C, ε_r values increased from 5.8 to 7.2 due to the increased relative density. Quality factor ($Q \times f$) values exhibit a similar trend with relative density of the samples as a function of sintering temperatures (Fig. 8(b)). The $Q \times f$ values increase with the growth grain size, but as the sintering temperature increasing up to 1100 °C the abnormal grain growth makes the $Q \times f$ values decrease. With increasing temperatures from 1000 to 1075 °C, the τ_f values very from −63 to −58 ppm/°C and the $Q \times f$ values increase from 74,800 to 193,800 GHz. The optimum $Q \times f$ value (193,800 GHz) is comparable with those achieved by a conventional solid state reaction method sintered at 1350–1550 °C [2,7].

4. Conclusions

The phase formation temperature of Mg_2SiO_4 nanopowders from MgO and SiO_2 was reduced about 300 °C by using HEBM. The lowered forsterite Mg_2SiO_4 phase formation temperature was attributed to the refinement of the oxides and mechanical alloying process. Mg_2SiO_4 powders with an average grain size of 147.4 nm were obtained by HEBM for 30 h and calcined at 850 °C for 3 h, 300 °C lower than required by a conventional solid state reaction method. The forsterite Mg_2SiO_4 ceramics from HEBM powders sintered at 1075 °C showed dense microstructures and excellent microwave dielectric properties ($\varepsilon_r = 7.2$, $Q \times f = 193{,}800$ GHz, $\tau_f = -58$ ppm/°C). It is believed that the HEBM technique can be extended to other microwave dielectric materials.

Acknowledgement

The work was supported by the National Natural Science Foundation of China (Grants Nos. 51072110 and 51132003).

References

[1] T. Sugiyama, T. Tsunooka, K. Kakimoto, H. Ohsato, J. Eur. Ceram. Soc. 26 (2006) 2097–2100.
[2] T. Tsunooka, M. Androu, Y. Higashida, H. Sugiura, H. Ohsato, J. Eur. Ceram. Soc. 23 (2003) 2573–2578.
[3] A. Stiegescjmitt, A. Roosen, C. Ziegler, S. Martius, L. Schmidt, J. Eur. Ceram. Soc. 24 (2004) 1463–1466.
[4] S. Ni, L. Chou, J. Chang, Ceram. Int. 33 (2007) 83–88.
[5] K.P. Sanosh, A. Balakrishnan, L. Francis, T.N. Kim, J. Alloys Compd. 495 (2011) 113–115.
[6] F. Tavangarian, R. Emadi, Mater. Lett. 65 (2011) 126–129.
[7] K.X. Song, X.M. Chen, X.C. Fan, J. Am. Ceram. Soc. 90 (2007) 1808–1811.
[8] L.B. Kong, T.S. Zhang, J. Ma, F. Boey, Prog. Mater. Sci. 53 (2008) 207–322.
[9] Z.F. Fu, P. Liu, X.M. Chen, J.L. Ma, H.W. Zhang, J. Alloys Compd. 493 (2010) 441–444.
[10] S.C. Prashantha, B.N. Lakshminarasappa, B.M. Nagabhushana, J. Alloys Compd. 509 (2011) 10185–10189.
[11] Y.C. Chen, Y.N. Wang, C.H. Hsu, J. Alloys Compd. 509 (2011) 9650–9653.
[12] M. Kharaziha, M.H. Fathi, Ceram. Int. 35 (2009) 2449–2454.
[13] S.B. Kim, S.J. Kim, C.H. Kim, W.S. Kim, K.W. Park, Mater. Lett. 65 (2011) 3313–3316.
[14] S. Sano, N. Saito, S. Matsuda, N. Ohashi, H. Haneda, J. Am. Ceram. Soc. 89 (2006) 568–574.
[15] D. Goeuriot, J.C. Dubois, D. Merle, F. Thevenot, P. Exbrayat, J. Eur. Ceram. Soc. 18 (1998) 2045–2056.
[16] A. Saberi, B. Alinejad, Z. Negahdari, F. Kazemi, A. Almasi, Mater. Res. Bull. 42 (2007) 666–673.
[17] M.F. Zawrah, Mater. Sci. Eng. A 382 (2004) 362–370.
[18] W.F. Giauque, Contribution from the chemical laboratory of the university of california 71 (1949) 3192.
[19] H. Ohsato, T. Tsunooka, Y. Ohishi, Y. Miyauchi, M. Ando, K. Kakimot, J. Korean Ceram. Soc. 40 (2003) 350–353.
[20] B.W. Hakki, P.D. Coleman, IRE Trans. Microwave Theory & Tech. MTT-8 (1960) 402–410.
[21] I.H. Jung, S.A. Decterov, A.D. Pelton, J. Eur. Ceram. Soc. 25 (2005) 313–333.
[22] L.B. Kong, T.S. Zhang, J. Ma, F. Boey, J. Eur. Ceram. Soc. 23 (2003) 2247–2256.
[23] L. Nedelcu, M.I. Toacsan, M.G. Banciu, A. Ioachim, J. Alloys Compd. 509 (2011) 477–481.
[24] X. Chen, H. Zhou, L. Fang, X. Liu, Y. Wang, J. Alloys Compd. 509 (2011) 5829–5832.
[25] M. He, Sh. Zhang, X. Zhou, B. Li, J. Wan, J. Alloys Compd. 509 (2011) 4260–4263.
[26] Y.B. Chen, J. Alloys Compd. 509 (2011) 2285–2288.
[27] J. Guo, D. Zhou, H. Wang, X. Yao, J. Alloys Compd. 509 (2011) 5863–5865.
[28] Z. Liang, L.L. Yuan, J.J. Bian, J. Alloys Compd. 509 (2011) 1893–1896.
[29] M.A. Sanoj, C.P. Reshmi, K.P. Sreena, M.R. Varma, J. Alloys Compd. 509 (2011) 3089–3095.
[30] L. Fang, D. Chu, H. Zhou, X. Chen, Z. Yang, J. Alloys Compd. 509 (2011) 1880–1884.
[31] A. Surjith, N.K. James, R. Ratheesh, J. Alloys Compd. 509 (2011) 9992–9995.
[32] M.K. Suresh, A. John, J.K. Thomas, P.R.S. Wariar, S. Solomon, J. Alloys Compd. 509 (2011) 2401–2406.
[33] S. Wu, J. Luo, J. Alloys Compd. 509 (2011) 8126–8129.